Pergamon

Geochimica et Cosmochimica Acta, Vol. 65, No. 18, pp. 3055–3063, 2001

0016-7037/01 $20.00 + .00

PII S0016-7037(01)00649-4

Point of zero charge of a corundum-water interface probed with optical Second Harmonic Generation (SHG) and Atomic Force Microscopy (AFM): New approaches to oxide surface charge

ANDREW G. STACK,[1,*] STEVEN R. HIGGINS,[1] and CARRICK M. EGGLESTON[1]

[1]Department of Geology and Geophysics, University of Wyoming, Laramie, WY 82071-3006 USA

(*Received January* 20, 2000; *accepted in revised form December* 1, 2000)

Abstract—The *p*H and ionic strength dependence of light generated at a corundum-solution interface by the nonlinear optical process of second harmonic generation (SHG) is reported. A point of zero salt effect occurs in the *p*H range 5 to 6. The *p*H and ionic strength dependence of the SHG is qualitatively consistent with a model describing SHG from a charged mineral/water interface from Ong et al. (1992) and Zhao et al. (1993a, 1993b), but certain aspects of the model appear inadequate to describe the full range of our data. Atomic force microscopy (AFM) force-distance measurements, though imprecise, were consistent with a point of zero charge (p.z.c.) for the interface also in the *p*H range 5 to 6. The SHG (and AFM) results are different from expectation; the observed p.z.s.e. (and presumably also the p.z.c.) is considerably lower than the accepted point of zero charge of clean alumina powders (*p*H 8–9.4; Parks, 1965; Sverjenksy and Sahai, 1996). Although the reasons for this are unclear, SHG holds promise as a probe of oxide-water interfaces that is independent of interpretation of acid-base titration stoichiometry. *Copyright © 2001 Elsevier Science Ltd*

1. INTRODUCTION

Chemical interaction between mineral surfaces and aqueous environments is of interest in understanding the chemistry of soils, aquifers and other near-surface environments. One important aspect of mineral-water interface geochemistry is the development of surface charge as a function of *p*H and electrolyte composition/concentration. Mineral surface charge affects partitioning of aqueous solutes between mineral surfaces and aqueous solution, the transport of aqueous ionic species through aquifers, interaction of particles in suspensions, and many other processes. Mineral surfaces develop charge in several ways, an important one being the adsorption of aqueous ions from solution (e.g., protons and counter ions of the electrolyte; Sposito, 1998).

It is widely accepted that H^+ and OH^- are potential determining ions (p.d.i.) for refractory metal oxides in aqueous solution (Parks, 1965, 1990; Stumm, 1992; Stumm and Morgan, 1996), and surface charge can thus be expressed as a function of *p*H. The point of zero net proton charge (p.z.n.p.c.) is defined as the *p*H at which surface sites with positive and negative charge developed by proton adsorption or desorption occur in equal numbers (Sposito, 1984). If there are p.d.i. other than H^+ and OH^-, a more generally defined *p*H of the point of zero charge (p.z.c.) can be defined that accounts for surface charge resulting from ions other than H^+ and OH^-. The p.z.n.p.c. and p.z.c. are important parameters for understanding the surface chemistry of minerals in aqueous solutions (Sposito, 1984, 1998; Stumm, 1992).

Mineral p.z.n.p.c. and p.z.c. are generally defined in relation to acid-base titrations of powder suspensions. From such stoichiometric data, surface potentials and thereby thermodynamic values such as *p*Ks for surface ionization can be extracted from models that relate surface charge density to surface potential (e.g., Parks, 1990; Hayes et al., 1991). It remains difficult to independently assess the applicability of particular models to specific situations because, for electrically insulating oxides, surface potential cannot be measured directly.

Mineral p.z.c. has been systematized using a solvation model incorporating the average bulk dielectric constant of the solid (Sverjensky, 1994; Sverjensky and Sahai, 1996). The dielectric constant is often an anisotropic property, and may be different at an interface than in either bulk phase. Different crystallographic surfaces may therefore have different characteristic p.z.c. values. As an example of crystallographically anisotropic adsorption, phosphate adsorption on aluminous hematites occurs preferentially on non-basal faces such that total adsorption capacity decreases as the ratio of the diameter to the thickness of the particles increases (Barrón et al., 1988; Colombo et al., 1994). Such structure-reactivity relations could be tested for proton sorption if there were a method for measuring the p.z.c. of specific crystal faces. Potentiometric titrations utilize powders to maximize mineral surface area, which generally does not allow for discrimination between different crystal faces (although one example of the use of microelectrode voltammetry has been presented; Unwin and Bard, 1992).

The work reported here represents a step toward developing methods that allow for both stoichiometry-independent assessment of surface potentials and for crystal-face specific measurement of p.z.c. values. We report the use of optical second harmonic generation (SHG) and atomic force microscopy (AFM) force-distance measurements to measure a point of zero salt effect (p.z.s.e.) and a p.z.c. for a corundum-water interface.

Corundum (sapphire; α-Al_2O_3) was chosen because aluminum (hydr)oxides are ubiquitous in soils and aquifers; although corundum is itself rare in low-temperature aqueous environments, it has been shown that surface sites readily hydroxylate to a gibbsite-like phase at water vapor partial pressures of ~1 Torr (Liu et al., 1998). Additionally, it is optically transparent

* Author to whom correspondence should be addressed (astack@uwyo.edu).

and available in relatively large crystals needed for SHG experiments. For these reasons, corundum is a defensible and frequently used proxy for aluminum (hydr)oxide phases that are more common in natural settings (e.g., O'Connor et al., 1956; Bargar et al., 1996; Elam et al., 1998).

2. SHG AT CHARGED INTERFACES

Second harmonic generation (SHG) has been used to gather information about adsorbate concentration and molecular orientation from a variety of optically accessible interfaces, including solid/liquid interfaces (see, e.g., Eisenthal, 1996). SHG is useful for the study of *p*H dependent surface properties because: 1) it is an in situ technique; 2) it can be inherently interface sensitive; and 3), its relatively small sampling area (approx. 1 mm^2) makes examination of individual crystal faces possible.

The electric field portion of light varies sinusoidally with time and can polarize the electron cloud within a molecule exposed to it. When the magnitude of the electric field is small, the electron cloud can be described as a perfect harmonic oscillator, i.e., as the magnitude and sign of the electric field change, there is a proportional change in the position of the electrons. If the incident light wave's electric field is large, the resultant polarization can be anharmonic and include a significant component with twice the incident light's frequency, called the second order polarization, $P^{(2)}_{2\omega}$. $P^{(2)}_{2\omega}$ is responsible for creating the second harmonic light, and can be described as:

$$E_{2\omega} \propto P^{(2)}_{2\omega} = \chi^{(2)}_{:} E_{\omega} E_{\omega} \tag{1}$$

where $E_{2\omega}$ is the second harmonic field strength at frequency 2ω, E_{ω} is the incident light field, and $\chi^{(2)}$ is the second order non-linear susceptibility:

$$\chi^{(2)} = n_s \langle \alpha^{(2)} \rangle \tag{2}$$

where n_s is the number of molecules giving rise to the SH and $\alpha^{(2)}$ is the second-order polarizability (or hyperpolarizability) of the molecules; $\alpha^{(2)}$ is a third rank tensor describing the hyperpolarizability of the molecules involved and reflects the ability of the molecules to generate second harmonic light as well as their average orientation (denoted by the brackets).

If only electric dipole terms are considered in the nonlinear polarization, second harmonic generation is forbidden in a centrosymmetric phase because the induced polarizations are equal in opposite directions and destructively interfere so that no net SHG occurs. However, at an interface between two centrosymmetric phases the inversion symmetry is broken and SHG is allowed. This imparts to SHG its inherent interface sensitivity in otherwise centrosymmetric systems.

Ong et al. (1992) measured SHG from an amorphous silica/water interface as a function of *p*H and ionic strength, and proposed a model in which $P^{2\omega}_{(2)}$ is the sum of a *p*H-independent "baseline" and a *p*H- and ionic strength-dependent component:

$$E_{2\omega} \propto P^{(2)}_{2\omega} = \chi^{(2)}_{:} E_{\omega} E_{\omega} + \chi^{(3)}_{\vdots} E_{\omega} E_{\omega} \Psi_0 \tag{3}$$

where Ψ_0 is the electric potential at the interface (the surface potential of the mineral), and $\chi^{(2)}$ and $\chi^{(3)}$ are the second- and third-order non-linear susceptibilities, respectively. The $\chi^{(2)}$ term is attributed to an interfacial source whose hyperpolarizability is independent of *p*H or ionic strength (Ong et al., 1992, Zhao et al., 1993a, 1993b). The $\chi^{(3)}$ term, considered in conjunction with the surface potential, creates an effective $\chi^{(2)}$ term that depends on the static electric field across the interface (Lantz and Corn, 1994). Ong et al. (1992) suggest that $\chi^{(3)}$ reflects the properties of water molecules in the diffuse layer oriented in the static (d.c.) electric field imposed by the charged surface.

Using sum frequency generation (SFG, a technique related to SHG in which photons of different frequency are combined) on an air/water interface in the presence of a charged surfactant adsorbate, Gragson et al. (1997) found that the sum frequency (SF) intensity is not directly proportional to the surface potential. The dominant portion of the SFG intensity increase is attributed to an increase in the alignment of potential-oriented water molecules. The potential-oriented molecules reach a maximum alignment before the maximum surface potential is reached, resulting in an asymptotic increase in signal with increasing surface potential (Gragson and Richmond, 1998a, 1998b; Gragson et al., 1997), rather than a linear increase as assumed by the Ong et al. (1992) model.

Zhao et al. (1993a) measured the ionic strength dependence of the SHG from two similar interfaces that had net positive and negative charge, and found that the direction of the ionic strength dependence reverses with the sign of the net charge of the interface. This is attributed to constructive or destructive interference between the $\chi^{(2)}$ and $\chi^{(3)}$ terms of Eqn. 3. When the average orientation of water molecules produces second harmonic light in phase with that produced by the $\chi^{(2)}$ term, there is constructive interference; destructive interference occurs when the $\chi^{(3)}$ term is out of phase with the $\chi^{(2)}$ term.

The idea of interference between the terms of Eqn. 3 is supported by Du et al. (1994), who show that the phase of the SFG signal in resonance with OH vibrations from an amorphous silica/water interface shifts 180° between high and low *p*H. Toney et al. (1994, 1995) show that there is a 1Å shift in the most probable positions of oxygens in H_2O molecules near a charged platinum electrode-water interface when the sign of the charge reverses. This indicates that H_2O molecules near the interface are probably reversing their orientation when the potential changes sign, creating the constructive or destructive interference with the $\chi^{(2)}$ term in Eqn. 3.

Here, we apply these models to a corundum-water interface. Our results are in qualitative agreement with Ong et al. (1992) and Zhao et al. (1993a, 1993b), but we find that we cannot arrive at Nernstian potentials in all cases using the model analytically. We believe that the reason is probably related to the nonlinear $E_{2\omega}$-surface potential relationship suggested by Gragson and others. We show that SHG can be used to locate a p.z.s.e. that should coincide with the p.z.c. of the interface, and thus that SHG could be used to measure the local p.z.c. of a single crystal face. As proposed by Ong et al. (1992) and by Zhao et al. (1993a, 1993b), this is a step toward measuring surface potential independently of an interfacial charge-potential model.

3. EXPERIMENTAL

3.1. SHG

Figure 1 is a diagram of the SHG experimental configuration. We used a Continuum Nd:YAG 10 Hz pulsed laser, with an optical para-

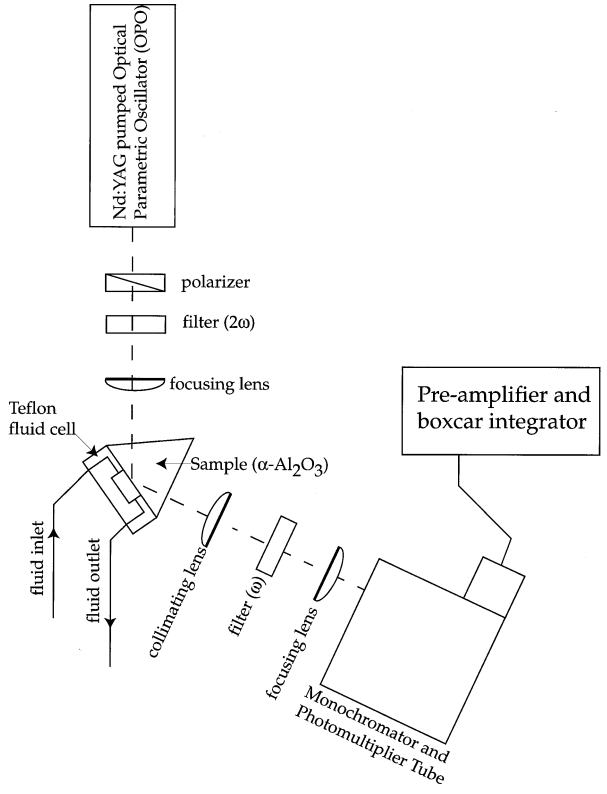

Fig. 1. Diagram of SHG experimental configuration. 1040 nm light from the idler channel of the OPO is focused on the corundum-water interface of the prism in TIR. The SH light is collected, counted and averaged using a photomultiplier tube and box car integrator connected to data acquisition software.

metric oscillator (OPO) set to output 1040 nm light (~10 mJ per pulse). The OPO output was focused on a single-crystal prism of corundum (Marketech International) in a total internal reflection (TIR) geometry; the fundamental light reflected off of the solid-water interface from the solid side of the interface. The prism was obtained with one side polished on the basal plane; although we did not confirm this orientation, AFM of this surface after annealing was consistent with the annealed morphologies of other basal-plane specimens. A continuous flow fluid cell was constructed so that the solution composition could be varied. When changing solutions, the *p*H of the effluent and influent were monitored to ensure adequate flushing of the fluid cell. SHG intensity was measured by focusing the SHG light (520 nm) on a monochromator, detected using a photomultiplier tube and averaged using a gated integrator and boxcar averager. Each data point shown here represents the mean of at least 500 samples. The error bars are minimum and maximum observed average SH field strengths, not standard deviations.

3.2. AFM

The roughness of the surface investigated with SHG was characterized by AFM. AFM imaging and force-distance measurements were performed using a Molecular Imaging PicoSPM run from a Digital Instruments Nanoscope IIIa controller. Force-at-contact (FAC) was determined using methods described by Eggleston and Jordan (1998). Silicon-nitride tips were used (Nanosensors) and presumed to be oxidized to mostly SiO_2 at the surface (Tsukruk and Bliznyuk, 1998; Arai and Fujihara, 1996). The mean FAC at each *p*H are reported here, with 2 to 15 individual measurements collected for each data point. Error bars are plus/minus two standard deviations of the average FAC.

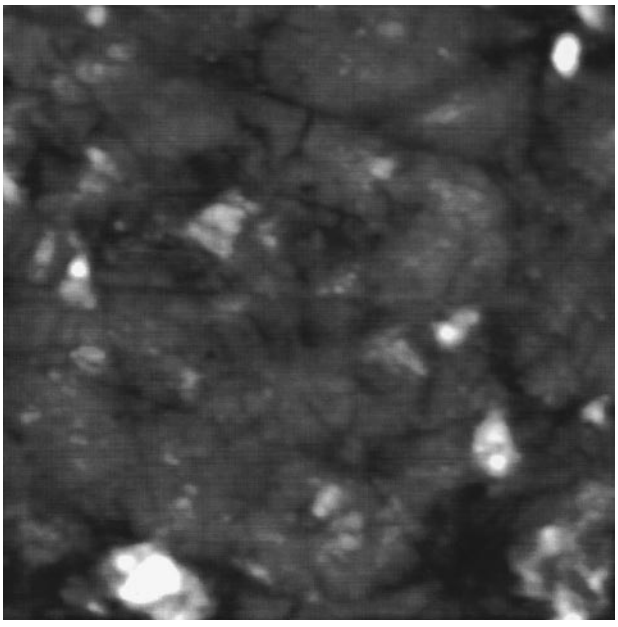

Fig. 2. AFM height image of the single-crystal corundum prism (3×3 μm). Z range is 57.7 nm. Numerous polishing scratches are visible.

3.3. Sample and Solution Preparation

Before placing in the fluid cell, the prism was sonicated in heated methanol and boiled in sulfuric acid for at least 30 min. All electrolyte solutions were made using 18.2 MΩ-cm distilled, de-ionized water and reagent grade chemicals. Sodium hydroxide and the acid of the anion in the electrolyte were used to modify the *p*H of the solutions.

Figure 2 shows an AFM image of the corundum prism surface. The surface roughness is dominated by polishing scratches. SHG data collected from this surface may thus not reflect a single crystallographic surface plane. Auger spectroscopy of the surface revealed only aluminum, oxygen and carbon (data not shown). All detectable carbon was removed by light Ar^+ sputtering (2 min at ~1.5 nm per minute), indicating minor, if any, diamond contamination from the polishing process.

After SHG and AFM experiments were carried out on the prism surface as shown in Figure 2, the prism was annealed. The prism was placed in a furnace at 500 °C, and the temperature was ramped to 1350 °C. Figure 3 shows the prism surface after annealing; relatively wide terraces have formed. SHG experiments were conducted immediately after annealing and again after allowing the prism to age in DI H_2O for periods of 5, 10 and 12 d. The step density was measured and it was determined that the surface was miscut by approximately 5° from the desired basal crystal face.

4. RESULTS AND DISCUSSION

4.1. SHG Field Strength vs. pH and Ionic Strength

The *p*H and ionic strength dependence of the SH field strength ($E_{2\omega}$) with $NaClO_4$, $NaNO_3$ and NaCl electrolytes are shown in Figure 4. At high (low) *p*H, SH field strength decreases (increases) with increasing ionic strength (Fig. 5). A point of zero salt effect (p.z.s.e.) occurs in the range of *p*H 5 to 6. According to the Ong et al. (1992) model, at the p.z.s.e. the diffuse layer contains no net charge and the $\chi^{(3)}$ term is zero because Ψ_0 is zero at this *p*H; the SH intensity should thus be due entirely to the $\chi^{(2)}$ term of Eqn. 3. When there is a potential difference across the interface, water molecules near the inter-

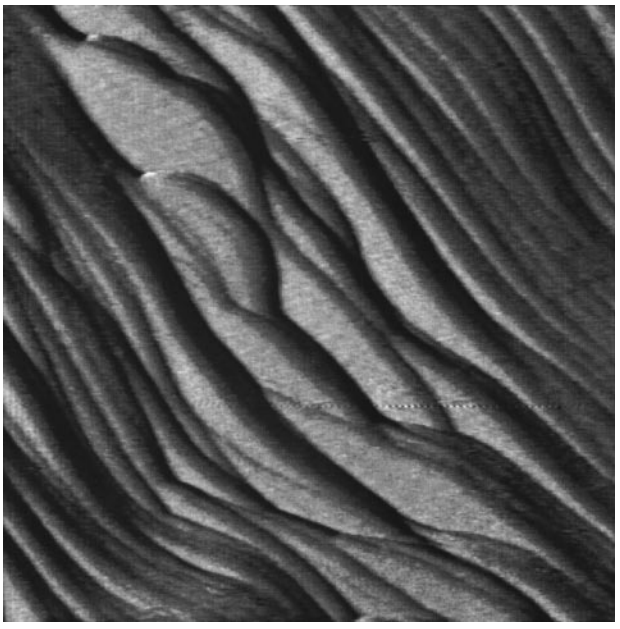

Fig. 3. AFM deflection image of the single crystal corundum prism after annealling (1.8 × 1.8 μm). Z range is 11.0 nm deflection; total topographic relief is 130 nm, stepping up from lower left to upper right. Relatively wide terraces slope downward from left to right at 5° to horizontal.

face are oriented such that their dipoles point, on average, either more towards or more away from the surface, depending on the sign of the surface potential. At *p*H > p.z.s.e., the average orientation of the potential-oriented water molecules ($\chi^{(3)}$ term) produce SH light that constructively interferes with the SH light attributed to the $\chi^{(2)}$ term in Eqn. 3. At *p*H < p.z.s.e., because the potential-oriented water molecules "flip" on average, there is destructive interference between the two sources. An increase in ionic strength decreases the magnitude of the $\chi^{(3)}$ term (because of the shortened diffuse layer and smaller potential difference), and will lead to an increase or decrease of the total SH signal, depending on whether there is constructive or destructive interference between the $\chi^{(2)}$ and $\chi^{(3)}$ terms.

The foregoing interpretation requires that the p.z.s.e. of the SHG coincides with the p.z.c. of the interface. The surface potential of the corundum must change sign at this *p*H because this is where the ionic strength dependence reverses direction. Corundum powders have generally been shown to have a p.z.c. in the *p*H range 8 to 9.4 (e.g., Parks, 1965, 1990; Stumm, 1992; Sverjenksy and Sahai, 1996), but because there is an ionic strength dependence in this *p*H region for the particular surface used in this study, the Ong et al. (1992) model would predict that the p.z.c. of the interface we used cannot be at such high *p*H. An adsorbed anion could be modifying the surface potential of the corundum (i.e., lowering the *p*H of the p.z.c.), but it is unlikely that this would change the p.z.c. as much as 2 to 5 *p*H units. The possibility that organic matter contaminates this surface so as to lower the p.z.s.e. is difficult to reconcile with the Auger spectroscopy data showing very little carbon on the surface.

4.2. AFM Force-Distance Measurements

AFM force-distance measurements were made (using the same corundum-water interface used in the SHG measurements) as a function of *p*H in 0.01 mol/L $NaNO_3$ as a means of independently confirming the SHG result (Fig. 6). According to Derjaguin-Landau-Verwey-Overbeek (DLVO) theory, there are two major forces acting between the tip and substrate: the Van der Waals (VdW) attraction and an electrostatic component (Hiemenz, 1977; McCormack et al., 1995). VdW forces are attractive and independent of *p*H or ionic strength. Their magnitude depends on such factors as tip shape and interaction area. When dealing with two substances of differing composition, i.e., a tip and substrate, the electrostatic component can be repulsive, attractive or zero. When the tip and substrate have significant charge of like sign, the electrostatic component will always be repulsive. Small amounts of surface charge (when VdW forces will dominate), or surface charge of opposite signs (providing an electrostatic attraction) will give a net attractive force at contact (FAC). Thus, the attractive FACs measured in the *p*H range 2 to 6 must mean that the p.z.c. of both the tip and the substrate (the corundum) are somewhere within this *p*H range (i.e., they both must be uncharged somewhere where the FAC is attractive). The large repulsive FACs measured near *p*H 8 to 9.5 show that the corundum surface must have substantial surface charge in this *p*H region. These results are thus inconsistent with a p.z.c. located in the *p*H range 8 to 9.5, regardless of the exact composition of the tip (or the presence of any kind of contamination on the tip).

We can further the interpretation of the results in Figure 6 by making some informed assumptions about the surface charge behavior of the tip: The silicon-nitride tips used were over two years old and expected to have oxidized to silica and behave as such with respect to their surface charge (Tsukruk and Bliznyuk, 1998). Amorphous silica has a p.z.c. at approximately *p*H 2 to 3.5 (e.g., Parks, 1965), and the majority of active surface sites deprotonate by *p*H 8.5 to 9.1 (e.g., Sverjenksy and Sahai, 1996; Ong et al., 1992), so that the surface approaches constant negative charge density above *p*H 10. Therefore, we expect that the average repulsive FAC between the tip and substrate at high *p*H indicates that both the tip and the surface have negative charge. At *p*H 8.5 to 9, the silica would begin to deprotonate and the magnitude of the repulsive FAC would increase, consistent with observation. In the *p*H range of 2.5 to 5, there is a small average attractive FAC. In this *p*H region, a silica-coated tip is expected to have a small negative charge, so the attractive forces are consistent with the alumina surface with a small positive charge. Finally, both the tip and surface are likely to have an average positive charge (and thus repel each other) at *p*H 2. Although the force-distance results are imprecise, they are consistent with a fundamental change in surface forces from repulsive to attractive as the *p*H decreases through the 5 to 6 region, which is the same region exhibiting a p.z.s.e. in the SHG data.

We can only speculate about why the p.z.c. indicated by these experiments and the literature p.z.c. values obtained from corundum powders are different. Here, the sampling area was nominally a basal plane of the corundum, but as shown in Figure 2, the polishing scratches and the 5° miscut roughen the surface (see above). The average p.z.c. of the crystal faces

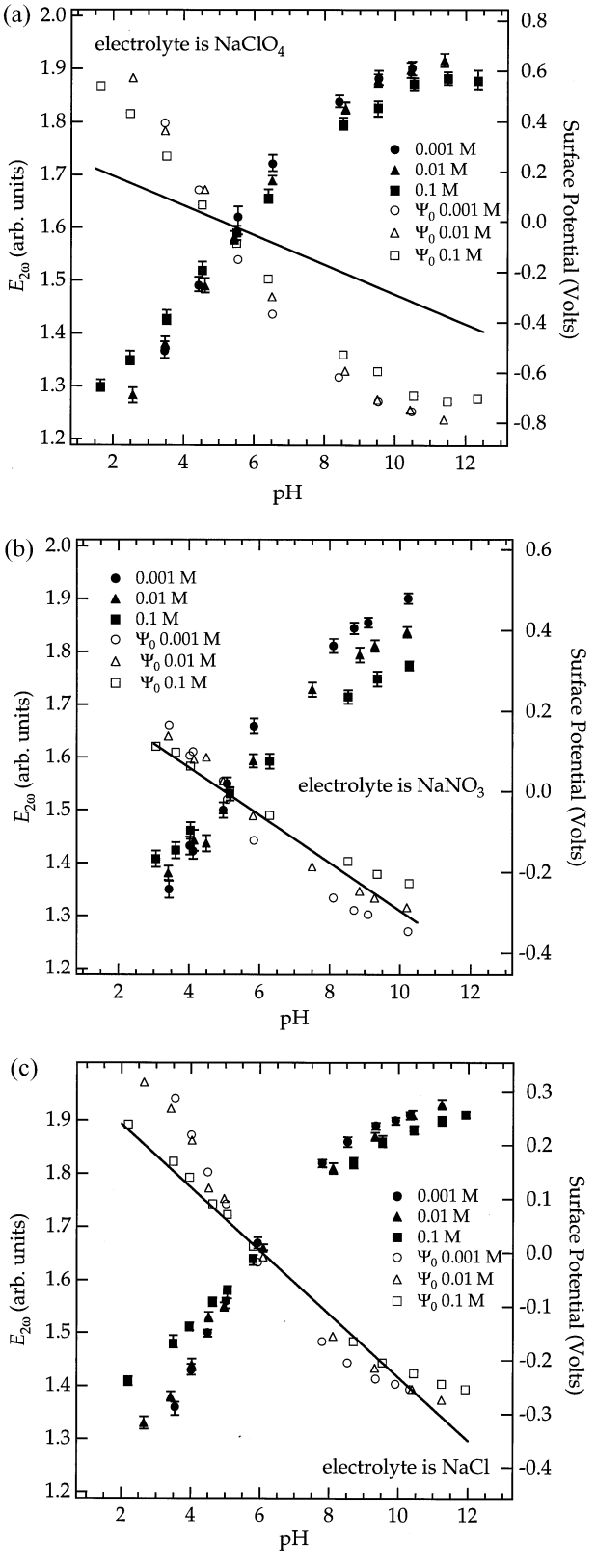

Fig. 4. $E_{2\omega}$ vs. *p*H, SHG from corundum-water interface with a) $NaClO_4$, b) $NaNO_3$ and c) NaCl as the electrolytes. Points of zero salt effect are near *p*H 5 to 6. Surface potentials were calculated using the Ong et al. 1992 model (see text). Solid line indicates a Nernstian slope, −59 mV/*p*H unit.

present in this nominal basal plane may differ from the average p.z.c. of a corundum powder. As mentioned previously, the dielectric constant is an anisotropic property, and different crystallographic surfaces may therefore have different characteristic p.z.c. values.

Furthermore, the exact composition of the surface sites may play a role in determining p.z.c. Robinson et al. (1965) found an isoelectric point (i.e.p.) for a freshly ignited (1400 °C) corundum powder near *p*H 6.7. The measured i.e.p. changed to *p*H 9.2 upon soaking in water for several days. As mentioned previously, the near surface corundum will readily hydroxylate to a gibbsite-like phase (Liu et al., 1998) which has a reported p.z.c. near *p*H 5.0 (Parks, 1965; Stumm and Morgan, 1981). Thus, the degree of surface hydroxylation of the corundum may also play a role in determining its p.z.c. At present, it is unknown how the kinetics of hydroxylation vary with crystal face and how fast a basal surface may hydroxylate to a gibbsite-like phase. During the course of our experiments the corundum prism was exposed to water for periods of much more than a week, sometimes months; therefore, the corundum surface is likely to have been hydroxylated (Liu et al., 1998) and perhaps behaved similarly to gibbsite.

4.3. SHG Models

Eqn. 3 (Ong et al., 1992) is approximated by using the following functionally equivalent expression (Zhao et al., 1993b):

$$E_{2\omega} = A + B\Psi_0 \tag{4}$$

where the magnitude of the fit parameters A and B are proportional to the second and third order non-linear susceptibilities ($\chi^{(2)}$ and $\chi^{(3)}$) and the square of the electric field strength vectors (E_ω) shown in Eqn. 3. If A and B are known, Eqn. 4 can be solved for surface potential. For each data set shown in Figure 4, the Guoy-Chapman model relating surface charge, σ_0, and surface potential, Ψ_0 (e.g., Sposito, 1984; Davis and Kent, 1990) was substituted for Ψ_0 in Eqn. 4:

$$E_{2\omega} = A + B\left[\frac{2RT}{F}\sinh^{-1}\left(\frac{\sigma_0}{\sqrt{8\epsilon_w RT}\sqrt{I}}\right)\right] \tag{5}$$

where I is the ionic strength and ε_w is the permittivity of bulk water. R,T and F have their usual meanings. According to the Guoy-Chapman model, when surface charge is a maximum (regardless of sign) it will not vary with ionic strength, due to saturation of available surface sites. Thus, if one measures the ionic strength dependence at a *p*H where surface charge is at a maximum, the only independent variable in Eqn. 5 is ionic strength. Estimates of A, B and σ_0 can be made by fitting such ionic strength dependence versus $E_{2\omega}$ (Fig. 5). Unfortunately, A and σ_0 are not always well constrained: A is determined by the SH field strength at the p.z.s.e. (i.e., $E_{2\omega\ \text{p.z.s.e.}} = A$), which is not always easily discerned from the data. This introduces significant uncertainty into the surface potential determination. Surface charge density was allowed to vary as long as it corresponded to a site density in the range 2 to 8 sites/nm^2, values that have been reported and used for α- and γ-alumina in the literature (corundum, 2 sites/nm^2: Sahai and Sverjensky, 1997; Yates et al., 1975. γ-alumina: ~8 sites/nm^2: Peri 1966,

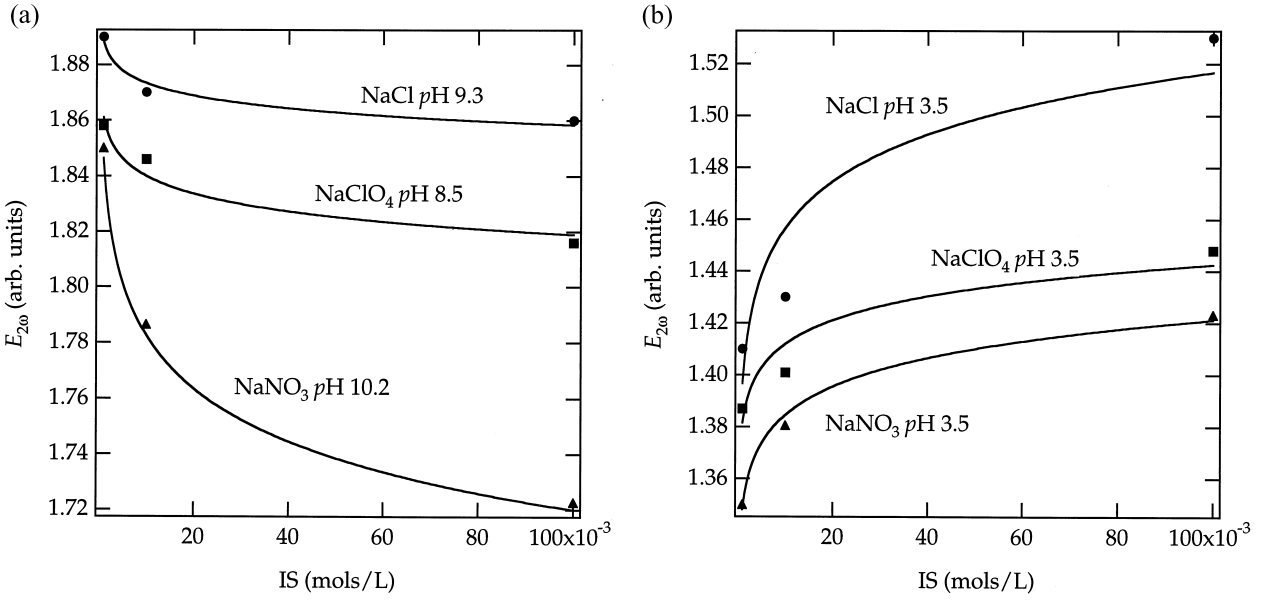

Fig. 5. Ionic strength dependence for $NaClO_4$, $NaNO_3$ and NaCl. At high *p*H, there is constructive interference between the $\chi^{(2)}$ and $\chi^{(3)}$ terms of Eqn. 3. At low *p*H, this dependence is reversed. Solid lines indicate fit to Eqn. 5. In the cases of $NaClO_4$ and NaCl, the low *p*H data was used to calculate the *B* and σ_0 parameters. For $NaNO_3$, the high *p*H data was used.

1965). Using the value of *B* determined for each electrolyte and a value of *A*, the surface potential can be calculated for the entire data set (Fig. 4). The next step is to examine the validity of the calculated surface potentials.

As a test of the surface potentials in Figure 4, the Nernst equation predicts that the slope of the measured Ψ_0 versus *p*H while surface sites are unsaturated (with respect to sorption reactions) must not be greater than 59 mV/*p*H unit. In the unsaturated regions of Figure 4 (approximately *p*H range 3 to 8 in our data), the maximum slope of the surface potentials are 185, 92, and 107 mV/*p*H unit (0.001 mol/L, Fig. 4a, b, and c, resp.) which clearly ranges from a little to a great deal too large to be Nernstian. This result does not imply that the surface is not behaving according to Nernst, but rather that the method used to determine surface potential is not universally applicable. Another test of the validity of the calculated potentials is to examine the difference between the minimum and maximum surface potentials at saturation. According to the DLM, the maximum magnitude of the surface potential should be determined by the surface site density and the ionic strength. Using a maximum surface site density of 8 sites/nm^2, and the lowest ionic strength (0.001 mol/L), the surface potential should not exceed $\pm$ 336 mV. Since the point of zero surface potential is not well defined here (see discussion on the *A* term of the Ong et al., 1992 model), we must use this as a maximum allowable range; the range of surface potentials should not exceed 671 mV. The surface potentials calculated for the sodium chloride and sodium nitrate fall within this range, but the sodium perchlorate potential range exceeds this number by more than 300 mV. From these two tests, it appears that, in these cases, the proposed SHG mechanism (Ong et al., 1992) may result in an overestimation of surface potentials; we will discuss some possible reasons for this below.

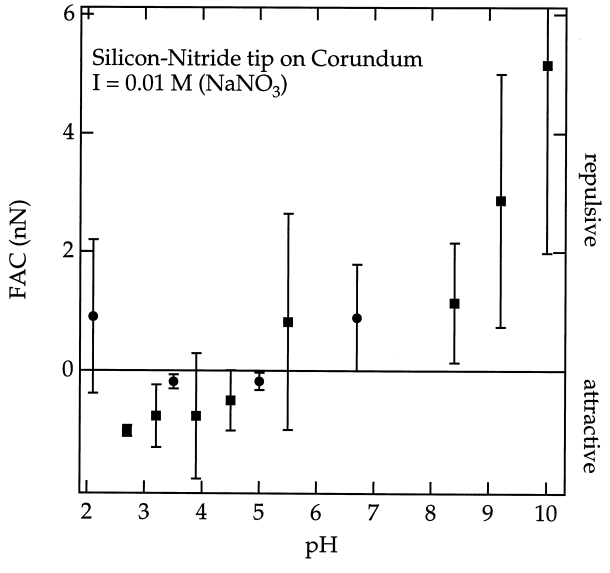

Fig. 6. Force at contact (see text) vs. *p*H for silicon-nitride tips on corundum. Circles and squares indicate measurements made with two different tips. Error bars indicate $\pm$ 2 standard deviations of the average measurement.

When determining the *B* fit parameter ($\chi^{(3)}$) for each data set, a *p*H must be chosen at which the surface charge is invariant with ionic strength. According to the Guoy-Chapman theory and the Ong et al. (1992) model, $E_{2\omega}$ should form a plateau in the *p*H region where surface sites have been saturated with respect to potential-determining-ion sorption reactions. In Figure 4, the *p*H regions with plateaus in $E_{2\omega}$ display minor ionic strength dependence. The size of the ionic strength dependence directly affects the magnitude of the *B* parameter that is used to calculate the surface potentials. If the estimation of *B* is too

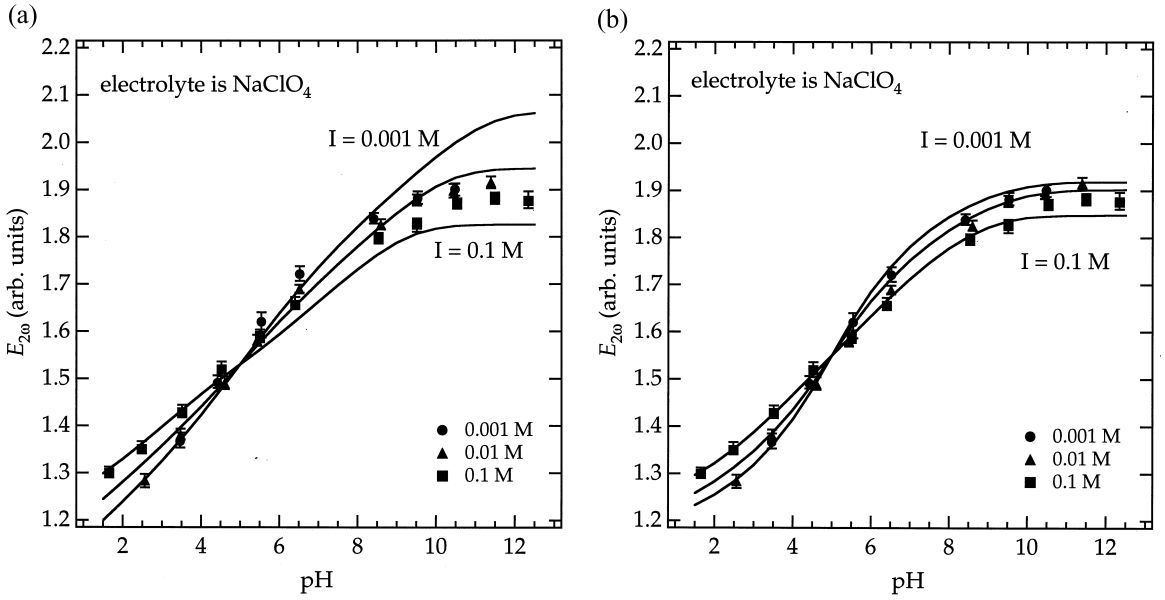

Fig. 7. $E_{2\omega}$ vs. *p*H, SHG from corundum-water interface with $NaClO_4$ as the electrolyte. a) $E_{2\omega}$ is calculated from surface potentials derived from a DLM and the Ong et al. (1992) model (Eqn. 3 and 4). The average chi-squared goodness-of-fit test statistic for the three ionic strengths is 0.0059. b) $E_{2\omega}$ is calculated from the same surface potentials as in a), but using a non-linear dependence of $E_{2\omega}$ on Ψ_0. The average chi-squared goodness-of-fit test statistic for the three ionic strengths is 0.0016.

small, the surface potentials will be overestimated. This is clearly demonstrated in the $NaClO_4$ data. In the cases of the sodium nitrate and sodium chloride data, the *B* parameter was estimated at a *p*H for which there was no plateau, but which showed the strongest ionic strength dependence (i.e., the largest *B* parameter). Since there is no plateau, surface charge is not a maximum and will vary with ionic strength. Therefore, the fitted *B* parameter will contain a systematic error due to variation of surface charge with ionic strength in addition to double-layer thickness; the $\chi^{(3)}$ estimation is thus inaccurate for these data by an unknown, but probably small, amount.

A more important consideration lies within form of the Ong et al. (1992) model itself; the approach is based on the assumption that the only surface potential dependent term in the total SH field strength is a $\chi^{(3)}$ term. Gragson and Richmond (1998a, 1998b) show that the TIR-SFG intensity of OH-bond stretches varies non-linearly with surface potential at a charged air/water interface, reaching a maximum at approx. 260 mV. It has been asserted that the interfacial water plays a dominant role in creating SHG from this interface (Zhao et al., 1994). If this is true, the intensities of the TIR-SFG, OH-bond stretches and the total TIR-SHG should behave similarly with changing surface potential (i.e., the Gragson and Richmond results should be applicable to our experiments). Therefore, a nonlinear dependence of $E_{2\omega}$ on surface potential is inconsistent with the assumption that a $\chi^{(3)}$ term is the only potential dependent term in the total SFG intensity.

At this point it is unclear how great a role potential dependent alignment of near-surface water molecules plays in our experiments, but the difference between our SHG-based estimates of surface potential as a function of *p*H and Nernstian behavior suggests that it may play a significant role. More accurate determination of surface potentials using SHG will require, therefore, a physical model of SHG from the oxide water interface that better incorporates the alignment of water molecules (and their ability to generate SH) within the diffuse layer as a function of surface potential.

We can attempt to explain why the Ong et al. (1992) model has worked well for estimating surface potential in some cases but not in others. From the Gragson (1997, 1998a, 1998b) results, $E_{2\omega}$ measurements at small surface potentials (i.e., less than approx. 230 mV) appear linear as a function of surface potential. In the case of amorphous silica, Ong et al. (1992) measure a maximum surface potential of ~140 mV at *p*H ~12.5. Because this potential is much smaller than that at which Gragson and Richmond's $E_{2\omega}$ vs. Ψ_0 results deviate from linearity, potentials calculated from the Ong et al. (1992) model may be accurate for experiments where surface potentials are relatively small. In our system, however, we may have larger surface potentials (i.e., where $E_{2\omega}$ vs. Ψ_0 deviates from a linear relationship). The Ong et al. (1992) model would then be expected to overestimate the "true" surface potentials, by (in this case) an unknown amount.

Unfortunately, due to the limited number of ionic strengths tested at any given *p*H (i.e., three), the method used above to determine surface potentials will not support any expansion in the number of variables used to describe the function which relates surface potential and $E_{2\omega}$. An alternate method is shown in Figure 7, where the surface potential was calculated beforehand from a homogenous, amphoteric surface site, diffuse layer model (DLM, e.g., Parks, 1990; Hayes et al. 1991) and fit to the SHG data from Figure 4a. Two *p*Ks for surface site proton sorption reactions were used, one at *p*H 3.5 and another at *p*H 6.5. The site density was fixed at 2.0 sites/nm^2 (Sahai and Sverjensky, 1997; Yates et al., 1975). The p.z.c. was fixed at *p*H 5 and the *p*Ks were determined by varying the ΔpK and

determining the goodness of fit using a chi-squared statistic. Figure 7a shows the Ong et al. (1992) model fits, which predict a greater ionic strength dependence than observed. This is in agreement with the considerations in the prior data treatment. Previously, we had calculated Ψ_0 as a function of the ionic strength dependence of $E_{2\omega}$ ($E_{2\omega}(I)$); here we are calculating $E_{2\omega}(I)$ from Ψ_0. If Ψ_0 is overestimated when calculated from $E_{2\omega}(I)$ in the first case, it follows that $E_{2\omega}(I)$ will be overestimated when calculated from Ψ_0.

Figure 7b shows a purely empirical, polynomial fit:

$$E_{2\omega} = A + B\Psi_0 + \mathrm{sgn}(\Psi_0)C\Psi_0^2 \quad (6)$$

where $\mathrm{sgn}(\Psi_0)$ is determined by the sign of the surface potential. This an empirical fit and is presented simply to show a nonlinear dependence of $E_{2\omega}$ on surface potential. While Eqn. 6 implies a higher order contribution to the surface non-linear susceptibility (χ_s), we are not intending to offer this as the sole explanation for the behavior of our data with respect to the Ong et al. (1992) model. The most likely explanation is that the A term is not independent of solution conditions and the variation in the A term contributes significantly to the $E_{2\omega}$. The total SHG intensity from the interface varies as some function of the surface charging properties of the interface, but at this point the exact functionality is unknown.

4.4. SHG Experiments after Annealing

After annealing, the magnitude of the SH signal as well as of the *p*H and ionic strength dependences were greatly diminished; with aging in water for a period of weeks, these signals were partly restored. These results are intriguingly systematic, but we cannot completely rule out the possible influences of drift in laser power or slight differences in experimental geometry from experiment to experiment (the prism was removed from the fluid cell for annealing and aging in water; because exact alignment is important in the TIR experimental geometry using anisotropic solids, comparing data across experiments is problematic).

However, if these results are due to the interface changing with annealing, they may indicate that the corundum surface itself contributes a non-negligible portion to the total SHG intensity. According to SHG theory, SHG is possible from any non-centrosymmetric medium, and an interface would contain non-centrosymmetric phases on either side of the water/alumina boundary. For this idea to be plausible, the nonlinear susceptibility of the surface sites would have to comparable to the nonlinear susceptibility of the interfacial water.

Another possibility is that the hydroxylation kinetics of the basal surface are very slow. The SHG signal was partially restored with aging in water. Due to the 5° miscut, there is a density of step-edges which may hydroxylate quickly (e.g., a period of days), yet the bulk of the sites present on the basal face may hydroxylate very slowly; this may explain why the signal was not restored fully. Further work is being conducted to confirm the apparent influence of surface microtopography, crystallographic structure/composition and the contribution of the corundum to the total SHG signal intensity.

5. CONCLUSIONS

SHG and AFM force-distance measurements at the corundum-water interface indicate a p.z.c. for the interface studied in the *p*H range 5 to 6. The Ong et al. (1992) model for SHG from a silica-water interface was unable to predict reasonable surface potentials from the SHG from our corundum-water interface in all cases, probably because of the assumption of a linear relationship between Ψ_0 and the SH intensity attributed to potential oriented water molecules near the charged oxide-water interface. Although more work is necessary, these results point intriguingly to the effects of crystallographic structure/composition on surface charge density and the structure of interfacial water.

Acknowledgments—This work was supported by the National Science Foundation under CHE-9708451 to SRH and CME, EAR-9875830 to CME, and by the Petroleum Research Fund, administered by the American Chemical Society, under Grant No. 32883-G2 to CME. We thank two anonymous reviewers for constructive comments, Dan Dessau, Kathy Nagy, and Boris Pinkhasov for arranging and conducting the Auger Spectroscopy, and Susan Swapp for X-ray diffraction work.

Associate editor: S. J. Traina

REFERENCES

Arai T. and Fujihara M. (1996) Effects of electric potentials on surfaces in electrolyte solutions. *J. Vac. Sci. Tech. B.* **14,** 1378–1382.

Bargar J. R., Towle S. N., Brown G. E. Jr. and Parks G. A. (1996) Outer-sphere Pb(II) adsorbed at specific surface sites on single crystal α-alumina. *Geochim. Cosmochim. Acta* **60,** 3541–3547.

Barrón V., Herruzo M. and Torrent J. (1988) Phosphate adsorption by aluminous hematites of different shapes. *Soil Sci. Soc. Am. J.* **52,** 647–651.

Colombo C., Barrón V. and Torrent, J. (1994) Phosphate adsorption and desorption in relation to morphology and crystal properties of synthetic hematites. *Geochim. Cosmochim. Acta* **58,** 1261–1269.

Davis J. A. and Kent D. B. (1990) Surface complexation modeling in aqueous geochemistry. In *Mineral-Water Interface Geochemistry* (eds. M. F. Hochella, Jr. and A. F. White) *Min. Soc. of Am., Rev. Mineral.* **23,** 177–260.

Du Q., Freysz E. and Shen Y. R. (1994) Vibrational spectra of water molecules at quartz/water interfaces. *Phys. Rev. Letters.* **72,** 238–241.

Eggleston C. M. and Jordan G. (1998) A new approach to pH of point of zero charge measurement: Crystal-face specificity by scanning force microscopy (SFM). *Geochim. Cosmochim. Acta* **62,** 1919–1923.

Eisenthal K. B. (1996) Liquid interfaces probed by Second-Harmonic and Sum-Frequency Spectroscopy. *Chem. Rev.* **96,** 1343–1360.

Elam J. W., Nelson C. E., Cameron M. A., Tolbert M. A. and George S. M. (1998) Adsorption of H_2O on a single-crystal α-Al_2O_3(0001) surface. *J. Phys. Chem. B.* **102,** 7008–7015.

Gragson D. E., McCarty B. M. and Richmond G. L. (1997) Ordering of interfacial water molecules at the charged air/water interface observed by vibrational sum frequency generation. *J. Am. Chem. Soc.* **119,** 6144–6152.

Gragson D. E. and Richmond G. L. (1998a) Investigations of the structure and hydrogen bonding of water molecules at liquid surfaces by vibrational sum frequency spectroscopy. *J. Phys. Chem. B.* **102,** 3847–3861.

Gragson D. E. and Richmond G. L. (1998b) Potential dependent alignment and hydrogen bonding of water molecules at charged air/water and CCl_4/water interfaces. *J. Am. Chem. Soc.* **120,** 366–375.

Hayes K. F., Redden G., Ela W. and Leckie J. O. (1991) Surface complexation models: An evaluation of model parameter estimation using FITEQL and oxide mineral titration data. *J. Coll. Interf. Sci.* **142,** 448–469.

Hiemenz P. C. (1977) Principles of Colloid and Surface Chemistry. Marcel Dekker, Inc., New York. pp 352–452.

Lantz J. M. and Corn R. M. (1994) Electrostatic field measurements and band flattening during electron transfer processes at single-crystal TiO_2 electrodes by electric field-induced optical second harmonic generation. *J. Phys. Chem.* **98,** 4899–4905.

Liu P., Kendelewicz T., Brown G. E. Jr. Nelson E. J. and Chambers S. A. (1998) Reaction of water vapor with α-Al_2O_3(0001) and α-Fe_2O_3(0001) surfaces: synchotron X-ray photoemission studies and thermodynamic calculations. *Surf. Sci.* **417,** 53–65.

McCormack D., Carnie S. L. and Chan D. Y. C. (1995) Calculations of electric double-layer force and interaction free energy between dissimilar surfaces. *J. Coll. Inter. Sci.* **169,** 177–196.

O'Connor D. J., Johansen P. G. and Buchanan A. S. (1956) Electrokinetic properties and surface reactions of corundum. *Trans. Farad. Soc.* **52,** 229–236.

Ong S., Zhao X. and Eisenthal K. B. (1992) Polarization of water molecules at a charged interface: Second harmonic studies of the silica/water interface. *Chem. Phys. Lett.* **191,** 327–335.

Parks G. A. (1965) The isoelectric points of solid oxides, solid hydroxides, and aqueous complex systems. *Chem. Rev.* **65,** 177–198.

Parks G. A. (1990) Surface Energy and adsorption at mineral/water interfaces: An introduction. In *Mineral-Water Interface Geochemistry* (ed. M. F. Hochella, Jr. and A. F. White); *Min. Soc. of Am., Rev. Mineral.* **23,** 133–169.

Peri J. B. (1966) Infrared study of adsorption of carbon dioxide, hydrogen chloride, and other molecules on "acid" sites on dry silica-alumina and γ-alumina. *J. Phys. Chem.* **70,** 3168–3179.

Peri J. B. (1965) Infrared and gravimetric study of the surface hydration of γ-alumina. *J. Phys. Chem.* **69,** 211–219.

Robinson M., Pask J. A. and Fuerstenau D. W. (1964) Surface charge of alumina and magnesia in aqueous media. *J. Am. Ceram. Soc.* **47,** 516–520.

Sposito G. (1984) The surface chemistry of soils. Oxford University Press, New York. p 78–93.

Sposito G. (1998) On points of zero charge. *Env. Sci. Tech.* **32,** 2815–2819.

Stumm, W. (1992) Chemistry of the solid-water interface. John Wiley and Sons, Inc. New York. pp 43–50.

Stumm W. and Morgan J. J. (1981) Aquatic Chemistry, 2nd edn, John Wiley and Sons, Inc.

Stumm W. and Morgan J. J. (1996) Aquatic Chemistry, 3rd ed., John Wiley and Sons, Inc.

Sverjensky D. A. (1994) Zero-point-of-charge prediction from crystal chemistry and solvation theory. *Geochim. Cosmochim. Acta* **58,** 3123–3129.

Sverjensky D. A. and Sahai N. (1996) Theoretical prediction of single-site surface-protonation equilibrium constants for oxides and silicates in water. *Geochim. Cosmochim. Acta.* **60,** 3773–3797.

Toney M. F., Howard J. N., Richer J., Borges G. L., Gordon J. G., Melroy O. R., Wiesler D. G., Yee D. and Sorenson L. B. (1995) Distribution of water molecules at Ag(111)/electrolyte interface as studied with surface X-ray scattering. *Surf. Sci.* **335,** 326–332.

Toney M. F., Howard J. N., Richer J., Borges G. L., Gordon J. G., Melroy O. R., Wiesler D. G., Yee D. and Sorenson L. B. (1994) Voltage-dependent ordering of water molecules at an electrode-electrolyte interface. *Nature.* **368,** 444–446.

Tsukruk V. V. and Bliznyuk V. N. (1998) Adhesive and friction forces between chemically modified silicon and silicon nitride surfaces. *Langmuir.* **14,** 446–455.

Unwin P. R. and Bard A. J. (1992) Ultramicroelectrode voltammetry in a drop of solution: A new approach to the measurement of adsorption isotherms at the solid-liquid interface. *Anal. Chem.* **64,** 113–119.

Yates D. E. (1975) The structure of the oxide/aqueous electrolyte interface. Ph.D. dissertation, Univ. Melbourne.

Zhao X., Ong S. and Eisenthal K. B. (1993a) Polarization of water molecules at a charged interface. Second harmonic studies of charged monolayers at the air/water interface. *Chem. Phys. Lett.* **202,** 513–520.

Zhao X., Ong S., Wang H. and Eisenthal K. B. (1993b) New method for determination of surface pK_a using second harmonic generation. *Chem. Phys. Lett.* **214,** 203–207.